Halogen bonds involved in binding of halogenated ligands by protein kinases

Jarosław Poznański[1,*], Maria Winiewska[1], Honorata Czapinska[1,2], Anna Poznańska[3], David Shugar[1,*]

[1]Institute of Biochemistry and Biophysics PAS, Pawińskiego 5a, 02-106 Warszawa, Poland

[2]International Institute of Molecular and Cell Biology, Trojdena 4, 02-109 Warszawa, Poland

[3]Centre for Monitoring and Analyses of Population Health Status, National Institute of Public Health - National Institute of Hygiene, Chocimska 24, 00-791 Warszawa, Poland

[*]jarek@ibb.waw.pl

Keywords: Halogen bonding, Protein kinase, Ligand binding, PDB screening

ABSTRACT

Analysis of 664 known structures of protein kinase complexes with halogenated ligands revealed 424 short contacts between a halogen atom and a potential protein X-bond acceptor, the topology and geometry of which were analyzed according to the type of a halogen atom (X=Cl, Br, I) and a putative protein X-bond acceptor. Among 236 identified halogen bonds, the most represented ones are directed to backbone carbonyls of the hinge region and may replace the pattern of ATP-like hydrogen bonds. Some halogen-π interactions with either aromatic residues or peptide bonds, that accompany the interaction with the hinge region, may possibly enhance ligand selectivity. Interestingly, many of these halogen-π interactions are bifurcated.

Geometrical preferences identify iodine as the strongest X-bond donor, less so bromine, while virtually no such preferences were observed for chlorine; and a backbone carbonyl as the strongest X-bond acceptor. The presence of a halogen atom in a ligand additionally affects the properties of proximal hydrogen bonds, which according to geometrical parameters get strengthened, when a nitrogen of a halogenated ligand acts as the hydrogen bond donor.

INTRODUCTION

Post-translational modifications (PTMs), both reversible and irreversible, may affect intracellular localization of proteins, regulate their interactions with protein or non-protein partners, modulate their catalytic activity, or select some of them for degradation. In general,

PTMs increase proteome diversity by at least an order of magnitude, when compared to the transcriptome, and even more so relative to the genome. They also enable rapid response or adaptation to extracellular factors, contributing to signal transduction and regulation of numerous cellular pathways. The most frequent modifications include glycosylation, lipidation, methylation, N-acetylation, S-nitrosylation and sumoylation. A particular role is played by reversible protein phosphorylation. The residues most susceptible to phosphorylation are serine, threonine and tyrosine, less frequently histidine (Klumpp & Krieglstein, 2002; Besant *et al.*, 2003; Steeg *et al.*, 2003; Besant & Attwood, 2005; Ciesla *et al.*, 2011), and rarely aspartate (Wagner & Vu, 2000; Lapek *et al.*, 2015), cysteine (Pannifer *et al.*, 1998; Feng *et al.*, 2008), lysine (Matthews, 1995; Khorasanizadeh, 2004; Besant *et al.*, 2009) or arginine (Fuhrmann *et al.*, 2009; Elsholz *et al.*, 2012). Protein kinases, which catalyze phosphorylation of proteins, display a large spectrum of substrate specificities. Most use ATP as a phosphate donor, albeit some may accept GTP (Ventimig & Wool, 1974).

Protein kinases are attractive molecular targets for drug design (Cohen, 2002), since they are playing key roles in the regulation of many cellular processes, including the cell cycle, growth and apoptosis. To date, most promising protein kinase inhibitors are small ATP-competitive molecules (Zhang *et al.*, 2009; Fabbro, 2015), which bind at the highly conserved ATP-binding site. To enhance target selectivity, some designed ligands are large enough to interact also with other functional sites of a kinase, i.e. bi-substrate inhibitors bind simultaneously at the ATP and substrate-binding sites (Parang *et al.*, 2001; Parang & Cole, 2002; Fischer, 2004; Gower *et al.*, 2014). Furthermore, some ligands forming a covalent bond with the kinase-specific nucleophilic residue located within the ATP-binding pocket have been developed (Liu *et al.*, 2013). Other options to improve selectivity include non-ATP-competitive inhibitors (Harrison *et al.*, 2008; Battistutta, 2009; Kirkland & McInnes, 2009; Garuti *et al.*, 2010), such as allosteric ones (Bogoyevitch & Fairlie, 2007; Lamba & Ghosh, 2012; Cowan-Jacob *et al.*, 2014), some of which preferably bind to the "DFG-out" conformation of a kinase, stabilizing its inactive conformation (Dietrich *et al.*, 2010; Zhao *et al.*, 2014).

Nonetheless, most of the currently used protein kinase inhibitors locate, at least partially, in the ATP-binding pocket. These ligands must mimic the overall properties of the ATP molecule, i.e. they are locally flat, preferably aromatic, and capable of hydrogen bond formation and efficient electrostatic interactions with residues that form the protein kinase ATP-binding site. According to the Lock-and-Key analogy originally postulated in 1894 by Fischer, and further extended to the Induced-Fit Theory (see Koshland, 1994 for review), which is a biochemical

equivalent of the Pauli exclusion principle: a low-mass ligand should fit to a binding site attainable for ligands in the solvent phase. Van der Waals (vdW) interactions, both attractive and repulsive, are short-range contacts that control binding events (Barratt *et al.*, 2005), favoring the ligands that fit to the protein binding site. Electrostatic interactions between a protein and a ligand are dominated by short contacts between charged groups (known as salt bridges, formally zero order term in multipole expansion of electrostatic interactions). Their contribution to the Gibbs free energy of ligand binding approaches 40 kJ/mol (Hendsch & Tidor, 1994). However, the subsequent moments in multipole expansion related to static (charge-dipole, dipole-dipole, etc) or induced-charge distributions (i.e. Debye and London forces), stacking interactions (electron correlation in proximal π-electron systems), hydrogen and halogen bonding, may also contribute significantly. The significance of these interactions is well described, with the exception of halogen bonding, the contribution of which is still under debate (Eckenhoff & Johansson, 1997; Liu *et al.*, 2005; Voth *et al.*, 2007; Memic & Spaller, 2008; Kraut *et al.*, 2009; Zou *et al.*, 2009; Hauchecorne *et al.*, 2010; Sarwar *et al.*, 2010; Carter & Ho, 2011; Hardegger *et al.*, 2011; Aakeroey *et al.*, 2013; Poznanski *et al.*, 2014), with estimates of the free energy of an individual X-bond varying from 0.8 (Sarwar *et al.*, 2010) up to 30 kJ/mol (Voth *et al.*, 2007).

Halogen bonding (X-bond) has been identified in many crystal structures of low-mass compounds and their supramolecular ensembles (see Metrangolo *et al.*, 2008 for review), and more recently in complexes of biomolecules with halogenated ligands (Auffinger *et al.*, 2004; Voth & Ho, 2007; Rendine *et al.*, 2011). Specific interactions between the ligand halogen atoms (Cl, Br, I) and the electron pairs of an oxygen/nitrogen/sulfur/π-electron system have been described, based largely on the observation that the distance between a halogen atom and its electron-donating partner, $d_{X\cdots Acc}$, is significantly shorter than the sum of their vdW radii (Figure 1A). Fluorine, because of its high electronegativity, is a very poor halogen bond donor (Politzer *et al.*, 2007), but it may act as an efficient hydrogen bond acceptor (Howard *et al.*, 1996; Dunitz, 2004)

The role of halogenated ligands in biological systems has been widely reviewed, amongst others by Auffinger *et al.*, 2004, Parisini *et al.*, 2011, Rendine *et al.*, 2011, Voth *et al.*, 2007, Voth *et al.*, 2009, Scholfield *et al.*, 2013, Wilcken *et al.*, 2013, Persch *et al.*, 2015 and also by us (Poznanski & Shugar, 2013; Poznanski *et al.*, 2014). These systematic structural studies show numerous examples of halogen bonds formed between a ligand and a protein electron-donating group. The geometry of these halogen bonds has been well described, with a

preference for the X···Acc-C (θ^A) angle of 160°, roughly resembling that of a hydrogen bond (Figure 1), albeit the distributions of θ^X and θ^D angles differ significantly. It should be however noted that the distribution of θ^A and θ^D angles depend on the hybridization of the involved atoms.

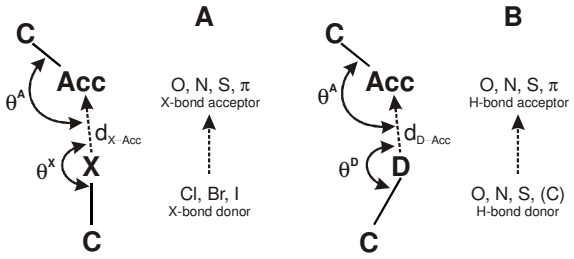

Figure 1. The structural analogy between a halogen (A) and a hydrogen (B) bond.

Numerous natural drugs (Smit, 2004; Wang *et al.*, 2005; Cabrita *et al.*, 2010) and an increasing number of synthetic drug candidates (Hernandes *et al.*, 2010; Pauletti *et al.*, 2010) are halogenated, comprising approximately 20% of low-mass protein ligands accessible in the Protein Data Bank (PDB), and an even larger number of tested protein kinase inhibitors. The growing number of high-resolution structures of protein kinase-ligand complexes aids *in silico* development of new inhibitors (Niefind *et al.*, 2009; Ibrahim, 2011; 2012; Lepsik *et al.*, 2013), many of them halogenated. Understanding the structural requirements for the binding of halogenated ligands, and the estimated contribution of the halogen bonding to the Gibbs free energy of ligand binding is crucial for *in silico* design of halogenated drugs (Ibrahim, 2012; Jorgensen & Schyman, 2012; Kolar & Hobza, 2012; Wang *et al.*, 2014).

Herein we present a detailed analysis of the geometry and topology of short contacts of halogen atoms identified in all complexes of protein kinases with halogenated ligands accessible in the Protein Data Bank. A statistical approach was applied to estimate, independently for Cl, Br and I as halogen bond donors, their relative contribution to the free energy of halogen bond formation in protein-ligand systems.

MATERIAL AND METHODS

Structural data. The Protein Data Bank (PDB) was searched to identify all entries of protein kinases (EC 2.7.10, 2.7.11 and 2.7.12), while histidine protein kinases (2.7.13) were omitted.

Structural analysis. All analyses were performed with the aid of the Yasara Model package (Krieger *et al.*, 2009). For each halogen atom type, all intermolecular ligand-protein contacts were identified, using 4 Å as a threshold for the distance between a halogen atom and a putative halogen bond acceptor. The analysis was further restricted to interactions characterized by the $d_{X\cdots Acc}$ distance between a halogen atom and a potential halogen bond acceptor shorter than the sum of their vdW radii. The contacts for which the C-X···Acc angle exceeded 140º (Figure 1) were annotated as halogen bonds. Multiple protein molecules in the unit cell, as well as objects displaying multiple partially occupied forms (i.e. side-chain rotamers or ligand locations) were analyzed separately.

Structure validation. The analysis was done with the aid of Coot (Emsley & Cowtan, 2004; Emsley *et al.*, 2010) and figures with the PyMol program (DeLano & Lam, 2005). Reliability of the presence, position and identity of solvent molecules in the vicinity of the halogen atoms was assessed in several ways. First, we eliminated all structures with resolution lower than 2 Å and structures with muliple conformations of the halogenated part of the ligand. Next, we manually inspected EDS- (Kleywegt *et al.*, 2004) and PDB REDO- (Joosten *et al.*, 2014) generated F_o-F_c (difference maps indicating disagreement between the observed, F_o, and calculated, F_c, electron densities) as well as $2F_o$-F_c electron density maps (maps calculated with model phases and experimental structure factors, with an additional F_o-F_c correction that counteracts the model bias). Finally we analyzed B-factors, coordination geometry and topology of the solvent molecules in question. Since there were only a few molecules fulfilling all selection criteria, we restricted solvent analysis to hi-res structures (<2.5Å) with deposed electron density maps, for which all solvent molecules in extremely short contacts with the halogen atoms (<2.5Å) were omitted. In all analyzed cases there were some ions of molecular weight comparable to water present in the crystallization buffer (Na^+, Mg^{2+} or NH_4^+). While metal ions should, in principle, be distinguishable from water on the basis of the coordination sphere, it is very hard to tell apart the ammonium ion and water based solely on crystallographic methods, and thus we cannot absolutely exclude the polar character of the identified interactions. X-ray radiation induced partial ligand decomposition also cannot be excluded.

Statistical analysis. To overcome the categorization issue, all distributions are presented in a cumulative manner as a CDF (cumulative distribution function), which is the integral of a commonly used distribution function. This form of presentation helps in visual comparison of various distributions of samples of a limited size. Since, according to the Anderson-Darling test (Anderson & Darling, 1952), most distributions were found to be non-Gaussian (data not

shown), the statistical significance of observed differences was estimated according to the Mann-Whitney U test (Mann & Whitney, 1947) for comparison of two datasets, and the Kruskal-Wallis H test (Kruskal & Wallis, 1952) for 3 or more groups. When the above tests did not show statistically significant differences in the location of the analyzed distributions, the Kolmogorov-Smirnov two-sample test, sensitive much more for the distribution shape, was applied (Massey, 1951). All analyses were performed using Statistica 10 (StatSoft, 2011). Null hypotheses that given distributions do not differ from each other were tested at a significance level of $\alpha = 0.05$, and those with p-values below 0.05 were rejected. The p-values listed in the text are indexed according to the applied method: p_{MW}, p_{KW} and p_{KS} for Mann-Whitney, Kruskal-Wallis and Kolmogorov-Smirnov test, respectively. In general, the distributions of $d_{X\cdots Acc}$ distance and C-X···Acc angle (judged by the smaller-larger principle), were preferably analyzed using Mann-Whitney or Kruskal-Wallis tests, and the X···Acc-C angle distribution, (interpreted in the wider-narrower terms), with the Kolmogorov-Smirnov two-sample test.

RESULTS AND DISCUSSION

Preferred topology of short contacts between a halogen atom of a ligand and a protein kinase. A total number of 424 short contacts between halogen atoms and potential X-bond acceptors was found in 320 of 664 structures of protein kinases in complexes with halogenated ligands. This includes 151 PDB records for protein-tyrosine kinases (Enzyme Classification 2.7.10), 386 for protein-serine/threonine kinases (EC 2.7.11) and 127 for dual-specificity protein kinases (EC 2.7.12). Short contacts were identified using thresholds calculated individually according to X-bond donor and acceptor types as the sum of their van der Waals (vdW) radii of 1.52, 1.55, 1.70, 1.75, 1.80, 1.85 and 1.98 Å for oxygen, nitrogen, carbon, chlorine, sulfur, bromine and iodine, respectively (Bondi, 1964). Overall, 223, 148 and 53 short contacts were identified for chlorine, bromine and iodine atoms attached to a carbon atom (halide ions were excluded from the analysis). This includes, respectively, 102, 88 and 46 interactions fulfilling distance and angle requirements for a halogen bond (Desiraju *et al.*, 2013). The numbers of identified short contacts and halogen bonds, are presented in Table 1. Only three of the highest populated X-bond acceptor types were present in sufficient numbers to assess the statistical significance of the observed halogen-dependent differences in the parameters describing the halogen bond geometry.

The most targeted protein kinase regions are the β-sheets of the N-terminal lobes, for which putative acceptors include both carbonyl oxygen and/or π-electrons of a peptide bond; and

carbonyls of residues located in the hinge region that are involved in the ATP binding (see Figure 2 below).

A carbonyl oxygen, in accordance with the PDB screenings (Auffinger *et al.*, 2004; Lu *et al.*, 2009; Hardegger *et al.*, 2011; Parisini *et al.*, 2011), is the most abundant putative acceptor of a halogen bond, contributing, together with an amide nitrogen, to over 50% of identified short intermolecular contacts. Due to geometrical reasons, most of the contacts between a halogen atom and a backbone nitrogen are accompanied by interaction(s) with a proximal carbonyl group. There are, however, some structures strictly representing the concept of orthogonal halogen bonds to π-electrons of the amide group, originally identified by Voth (Voth *et al.*, 2009). In the complex of human CDK2 with a brominated triazole-pyrimidine inhibitor (pdb2c69; Richardson *et al.*, 2006), the separate X-bond to the backbone nitrogen of Glu12 could be identified (Figure 2A), while in the complex of epidermal growth factor receptor variant with PD168393 (pdb4lrm; Yasuda *et al.*, 2013) the bromine atom makes numerous short orthogonal contacts with X-bond acceptors located in the proximal β-sheet (Figure 2B).

Interestingly, the side chain of aspartate located in the DFG loop may also interact with a halogen atom. This interaction has been rarely identified in the PDB records (Lu *et al.*, 2009; Wilcken *et al.*, 2013). However, there are nine PDB structures of protein kinases that display short contacts between a halogen atom and the carboxyl group of the aspartate located in the DFG motif: CK2α (pdb1zoh; Battistutta *et al.*, 2005, pdb4bxa, pdb4bxb, pdb4kwp; Cozza *et al.*, 2014), mitogen-activated kinases MAPK14 (pdb3fsf; Goldstein *et al.*, 2011) and MEK1 (pdb4u7z; Robarge *et al.*, 2014, pdb3eqc; Fischmann *et al.*, 2009), BTK kinase (pdb3pj1; Kuglstatter *et al.*, 2011), and serine/threonine protein kinase 10 (pdb4bc6), in most of which the orientation of a C-X bond relative to the proximal carboxyl group deviates from linearity by approximately 40º (Figure 2CD).

Figure 2.

Halogen bonding to the π-electron system of an aromatic residue. Protein kinase sequences show that each includes many aromatic residues, some of which are involved in catalysis, either by direct binding of ATP or transfer of the phosphate group. Those located in the vicinity of the ATP-binding site may form short contacts with halogenated ATP-competitive ligands. The

conserved aromatic residues in protein kinases are generally found in the glycine-rich loop (Y50 in CK2α/Y15 in CDK2), hinge region (F113/F80 and Y115/F82), catalytic loop (H154/H125 and H160/Q131), and the DFG-motif (W176/F146). Locations of aromatic residues for protein kinase CK2α are shown in Supplementary Figure 1. Interestingly, the aromatic residues are not strongly conserved in protein kinases and thus may be targeted by X-bonding to enhance ligand specificity.

Halogen bonding to π-electron systems is well documented in the Cambridge Structural Database (CSD), however only several structures demonstrating interactions between halogen atoms in organic systems and aromatic groups, the separation of which is shorter than the sum of their van der Waals radii, have been reported (Reddy *et al.*, 1996; Hubig *et al.*, 2000). Halogen bonds to π-electron systems have also been identified in complexes of halogenated ligands with various proteins, e.g. serine protease Xa (Nazare *et al.*, 2005), farnesyltransferase (Tong *et al.*, 2003), or HIV-1 reverse transcriptase (Das *et al.*, 2004).

Three modes of interaction between a halogen atom and an aromatic system have been identified, based on the orientation of the aromatic ring with respect to a C-X bond, which can be positioned either perpendicular or parallel to the normal vector defined by the plane of the aromatic ring. When a C-X bond is perpendicular to the plane of an aromatic ring (i.e. parallel to the normal vector), the halogen atom may interact either with the center of the π-electron system (Figure 3A) or with its rim (Figure 3B). The mode in which the C-X bond lies over the plane of the aromatic ring (Figure 3C), does not fulfill the formal geometrical requirements for halogen bonding, since the σ-hole, located along the C-X axis (Clark *et al.*, 2007), is not directed toward the potential halogen bond acceptor. When a halogen atom is attached to an aromatic moiety, possible π-π stacking interactions additionally compete with a halogen atom for a proximal π-electron system (Li *et al.*, 2012).

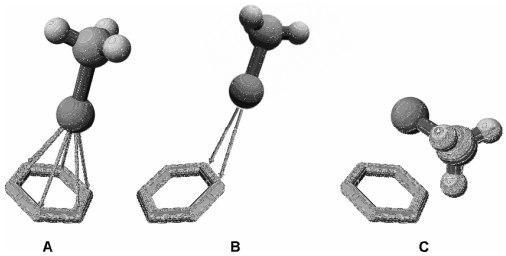

Figure 3. Schematic representation of perpendicular "over the center" (A), "over the rim" (B) and parallel (C) orientations of bromomethane relative to a proximal benzene aromatic ring.

Screening of structures of protein kinases in complexes with halogenated ligands has evidenced numerous close contacts between halogen atoms and π-electron systems. Their topology varies, but several classes can be identified. The most abundant short contacts with halogen atoms involve the phenylalanine residue of the hinge region (F113 in CK2α), next is a tyrosine residue located in the glycine-rich loop (Y50), and an aromatic residue from the DFG motif (W176). All structures that display short contacts between a halogen atom and an aromatic ring are collected in Table 2. The representative geometries are shown in Figure 2E-L. It should be noted, however, that the orientation of a C-X bond relative to a proximal aromatic ring for numerous identified systems disagrees with the idealized geometry of a halogen bond (see Figure 3AB). Thus, the halogenated ligand may be involved in a canonical π-π interaction with protein aromatic residue, as shown in Figure 2EF for chlorinated and brominated ligands (1RU with hepatocyte growth factor receptor in pdb4knb (Steinig *et al.*, 2013) and TV4 with serine/threonine-protein kinase B-Raf in pdb3tv4 (Wenglowsky *et al.*, 2011), respectively).

In numerous structures, the C-X···Acc angle differs substantially from the range of 160-180° found optimal in CSD (Rosokha & Kochi, 2008), as shown in Figure 2GH for RTX with serine/threonine-protein kinase pim-1 (pdb4med) and Z21 with subunit alpha of cAMP-dependent protein kinase (pdb4c37; Couty *et al.*, 2013). The largest number of short contacts with strongly perturbed geometry is observed for chlorinated ligands (>60% of all identified), in contrast to brominated and iodinated ones, for which the geometry close to optimal is preserved in the majority of analyzed cases (95 and 100%, respectively). Finally, a total number of 24 halogen bonds to π-electron aromatic systems, for which all geometrical requirements for efficient halogen bonding are fulfilled, have been identified (Table 2 and Figure 2I-L).

The halogen bond with the phenylalanine of the hinge region is often accompanied by two parallel hydrogen bonds formed with the backbone of the downstream residue (Phe+3), that for polyhalogenated ligands may be substituted by halogen bond(s) to the carbonyl groups of residues (+1) and (+3) (Figure 2JL). Alternatively, a halogen-π interaction may involve an aromatic residue of the glycine-rich loop, as observed in the complexes of mitogen-activated protein kinase 1 with E57 (pdb4fv6) or VTX-11e (pdb4qte; Chaikuad *et al.*, 2014), and cAMP-dependent protein kinase with H-89 (pdb3vqh; Pflug *et al.*, 2012) or CCT196539 (pdb4c37; Couty *et al.*, 2013). All these ligands also make hydrogen bond(s) with the (+3) residue of the hinge region.

Interestingly, a C-X···π halogen bond is frequently accompanied by a parallel interaction of the halogen atom with a proximal solvent molecule, identified in over 50 percent of the

analyzed structures (see Table 2). For ligands forming an X-bond with the hinge region, location of this solvent molecule is highly conserved, and the distance between the halogen atom and the oxygen atom (in case this solvent molecule is interpreted as water) is substantially shorter than the vdW limit. This may represent a possible example of a bifurcated halogen bond identified in crystals of small organic compounds (Lu *et al.*, 2006; Carlsson *et al.*, 2015; Novak *et al.*, 2015). The observed C-X···O_{wat} angle of approximately 120° (see Table 2) strictly corresponds to a minute maximum identified in the distribution of the C-X···O angles by Scholfield (Scholfield *et al.*, 2013), however it seems to be too far from the optimal 160-180° found for a plausible halogen bond in previous screenings of the PDB (Auffinger *et al.*, 2004; Parisini *et al.*, 2011; Poznanski & Shugar, 2013; Scholfield *et al.*, 2013) and CSD (Metrangolo *et al.*, 2005). Solvent molecules proximal to an X-bond have also been identified in other protein-ligand complexes (Beale *et al.*, 2013), but this type of three-body interaction has to date not been listed in the IUPAC definition of a halogen bond (Desiraju *et al.*, 2013). Moreover, a water molecule itself does not fulfill the actual IUPAC definition of an X-bond acceptor.

Halogen bond between a ligand and the backbone carbonyl oxygen. The shortest distances between a halogen atom and the carbonyl oxygen are observed for bromine (median of 3.19 Å calculated for all halogen-oxygen contacts shorter than 3.5 Å, see Figure 4I), whereas, notwithstanding the large difference in vdW radii, the distributions for chlorine and iodine donors are almost identical (medians of 3.25 and 3.28 Å, respectively). This, in view of the vdW radii (1.52, 1.75, 1.85 and 1.98 Å for O, Cl, Br and I, respectively), denotes that medians for Br and I are smaller than the sum of the corresponding vdW radii by approximately 0.2 Å, indicative of a halogen bond formation (Desiraju *et al.*, 2013). Figure 4A shows the distributions of what we refer to as the "void" distance $\Delta d_{X\cdots O}$, i.e. shortening of halogen to oxygen distance relative to the vdW radii sum, calculated for all structures for which $\Delta d_{X\cdots O} < 0$.

Figure 4.

The distribution of halogen-to-oxygen distances shows that the interaction between a chlorine and a carbonyl oxygen is substantially weaker than for bromine and iodine, i.e. $\Delta d_{Cl\cdots O}$ is less negative than $\Delta d_{Br\cdots O}$ and $\Delta d_{I\cdots O}$ (p_{MW} = 0.003 and 0.03, respectively), which do not differ from each other significantly ($p_{KS} > 0.1$, solid lines in Figure 4A). Correspondingly, θ^X (C-X···Acc) and θ^A (X···Acc-C) angles, which define the geometry of an X-bond, differ

qualitatively (Figure 4BC). For iodine, the distribution of θ^X is indicative of formation of the halogen bond, while for chlorine and bromine it is much more broadly distributed ($p_{MW}=3\cdot10^{-11}$ and $9\cdot10^{-7}$), with minimal difference between the two ($p_{MW} > 0.3$; $p_{KS} < 0.1$). Moreover, in contrast to iodine, for chlorine and bromine in approximately 25% of structures the θ^X angle is smaller than the assumed limit of 140º, and in only about a half of all cases falls within the optimal range of 160-180º (Figure 4B).

The sharp maximum in the θ^A (X···Acc-C) distribution for iodine, observed as the upcast in the cumulative distribution at 126º (Figure 4C), coincides with the halogen-oxygen orientation optimal provided the spatial distribution of electron density of oxygen in sp^2 hybridization. The same effect can also be observed for 40% of carbonyl-bromine contacts (θ^A ~ 133º), and less evidently for 20% of carbonyl-chlorine interactions. It should be noted that, despite the minute differences in location, these distributions differ significantly in the shape ($p_{KS} < 0.03$ for Cl vs. Br, and $p_{KS} < 0.001$ for I vs. Br/Cl). Consequently, much more narrower distributions are indicative for stronger halogen-carbonyl interaction, i.e. iodine is significantly better X-bond donor than bromine, while virtually no preferences are observed for chlorine. These is better visible, when the restricted set of contacts with θ^X>140º was analyzed, as it is evidenced by chopped lines in Figure 4A-C, however due to decreased number of analyzed structures, the differences in distributions are less significant.

Statistically, a halogen bond between a carbonyl oxygen and iodine is stronger than that between a carbonyl and bromine, geometry of which is less restricted to values optimal for a halogen bond ($\theta^X\approx$160-180º and $\theta^A\approx$120-160º), while virtually no propensity for halogen bonding is observed for chlorine.

Short contacts between a halogen atom of a ligand and a side-chain oxygen. There are no halogen-type specific differences in either distance or angle distributions of short contacts between a halogen atom and a side-chain oxygen (in all cases $p_{KS} > 0.1$, Figure 4D-F). Moreover, the angular preferences of such contacts differ, for each halogen type tested, from that made with a backbone carbonyl (in all cases $p_{MW} < 0.03$, Figure 4BC vs. 4EF), clearly confirming that the backbone carbonyl is a stronger X-bond acceptor than a side-chain oxygen. These differences cannot be explained by heterogenic hybridization of side-chain oxygen atoms (sp^2 for Asn, Asp, Gln and Glu, and sp^3 for Ser, Thr, Tyr). However, the differences observed for distance distributions are not significant (only for chlorine $p_{MW} < 0.05$, Figure 4A vs. 4D).

Short contacts between a halogen atom and a solvent molecule. The distance distribution between a halogen atom and a proximal solvent molecule resembles trends found for a carbonyl

oxygen acting as an X-bond acceptor ($p_{KS} > 0.1$, Figure 4G vs. 4A), however the distribution of the θ^X (C-X···O) angle is visibly broader (for each halogen type $p_{MW} < 0.0003$, Figure 4H vs. 4B). Contrary to the conclusions for contacts with side-chain oxygen, the distance preferences for θ^X angle depend of the halogen type, and for chlorine are weaker than for the other ones ($p_{MW} = 0.02$ and 0.10 for Cl vs. Br and I, respectively). It follows that, if solvent molecules were correctly identified as water, some of them may be regarded as a weak, but noticeable, X-bond acceptors (Figure 2R-T).

Halogen vs. hydrogen bonding in protein kinase-ligand complexes. Interestingly, the geometry of a halogen bond involving a backbone carbonyl of a protein kinase visibly differs from that observed for a hydrogen bond formed between a backbone carbonyl of a protein kinase and a nitrogen of either halogenated or non-halogenated ligand. The largest differences concern distance between a halogen atom and a carbonyl acceptor, which is approximately 0.3 Å larger than the nitrogen to oxygen distance of 2.87 Å observed for a hydrogen bond, which precisely corresponds to the difference in radii between N and X (see Figure 4I). Broad distributions of the θ^A angle for halogen bonds are shifted toward the idealized value of 120°, significantly differing from that observed for an H-bond ($p_{MW} < 10^{-8}$, chopped lines in Figure 4C), clearly indicating that the geometry of an X-bond is much more restricted. Moreover, θ^X qualitatively differs from θ^D (see Figure 1 for definitions), approaching the expected linear configuration for C-X···O, while for C-N···O angle of 120° is favored for ligand nitrogen, found mostly in sp^2 hybridization, acting as an H-bond donor. (chopped lines in Figure 4B).

Resuming, despite the general topological similarity of a halogen and hydrogen bond, geometrical requirements for both are visibly different, so they may not be equivalent when ligands are tightly packed inside the ATP-binding cavity of a protein kinase. A significant contribution of vdW interactions between atoms neighboring donor and acceptor sites, results in systematic deviation of θ^A from its optimal value of 120°, expected for the sp^2 hybridization of the carbonyl oxygen.

The most known example of a replacement of an H-bond by an X-bond is observed in the recurring pattern of two halogen bonds with backbone carbonyls in the hinge region, which resembles the common mode of ATP-recognition by a protein kinase (pdb1hck; Schulze-Gahmen *et al.*, 1996, Figure 2Q vs. 2M).

Hydrogen bonds formed by halogenated ligands. More detailed analysis shows that the presence of a halogen atom in the ligand affects the geometry of hydrogen bonds that it forms. The effect is less pronounced for the cases, when a ligand oxygen forms an H-bond with a

protein backbone amide than for those, in which backbone carbonyl acts as an H-bond acceptor (Figure 4M-O and 4J-L, red and blue lines vs. black ones). Small differences are observed for N···O distance distributions (Figure 4J and 4M, red vs. black lines), but variations in θ^D (Figure 4K,N) and θ^A (Figure 4L,O) are even more remarkable. All these differences are indicative of enhancement of the strength of a hydrogen bond. They are statistically significant when a nitrogen of a halogenated ligand acts as an H-bond donor (Figure 4J-L; $p_{KW} < 0.05$), but not for those in which a ligand oxygen acts as an H-bond acceptor (Figure 4M-O; $p_{KW} < 0.05$ only for angle C-O···N). The foregoing supports the trend of H-bond strengthening for halogenated ligands carrying a nitrogen H-bond donor, identified in a larger set of PDB structures (Poznanski *et al.*, 2014), however it is worth noting that the geometry of an H-bond, in which a ligand oxygen is the acceptor, is closer to the idealized geometry than that when a ligand donates an H-bond (Figure 4O vs. 4K, $p_{KW} < 0.01$).

Electrostatic contribution to ligand binding. Structure-activity screening of halogenated benzimidazole derivative inhibitors revealed a reasonably good correlation between the inhibitory activity and the change of ligand solvent-accessible surface upon binding (Battistutta *et al.*, 2007), which is indicative of predominance of hydrophobic interactions. However, comparison of binding modes of tetrabromobenzotriazole (TBBt) by two closely related protein kinases: CDK2 (pdb1p5e; De Moliner *et al.*, 2003) and CK2α (pdb1j91; Battistutta *et al.*, 2001) clearly shows that small differences in charge distribution may result in an alternative mode of TBBt binding (Figure 2MN). Similarly, three structurally related ligands: TBBt, tetrabromobenzimidazole (K17, TBBz, pdb2oxy; Battistutta *et al.*, 2007) and pentabromoindazole (K64, pdb3kxg; Sarno *et al.*, 2011) bind to CK2α in different orientations (Figure 2N-P). However, the poses for TBBt with CDK2 and TBBz with CK2α are almost identical (Figure 2M vs. 2O). Altogether, the analysis of protein kinase complexes with halogenated benzimidazoles suggests that subtle electrostatic interactions contribute substantially to ligand binding.

We have systematically explored electrostatic contribution to ligand binding by analyzing the structure-activity relationship for a series of TBBt derivatives (Wasik *et al.*, 2010), in which the Br at C(5) of TBBt is replaced by various groups differing in their physicochemical properties, and also for a series of nine bromobenzotriazoles representing all possible patterns of halogenation on the benzene ring (Wasik *et al.*, 2012a). Overall, the hydrophobicity of the monoanionic form of the ligand appeared to be the principal factor governing its inhibitory activity against CK2α (Wasik *et al.*, 2010; Wasik *et al.*, 2012b). Furthermore, the moderate

inhibitory activity exhibited by 4,5,6,7-tetramethylbenzotriazole (Zien *et al.*, 2003), which in contrast to TBBt is in the neutral form at physiological pH (Poznanski *et al.*, 2007), again points to a balance of electrostatic and hydrophobic interactions as an important factor contributing to CK2α inhibition. Accordingly, recent DSC-derived thermodynamic data for binding of TBBt, TBBz and their close structural analogues to CK2α (Winiewska *et al.*, 2015a; Winiewska *et al.*, 2015b) confirm the predominant contribution of electrostatic and hydrophobic interactions. For ligands that are mostly dissociated (i.e. pK_a<6.5), the aqueous solubility and pK_a for dissociation of the triazole proton together account for more than 95% of the variance of the free energy of binding determined with the aid of Microscale Thermophoresis (Figure 5). Three remaining, less dissociated ligands, 4-bromobenzotriazole, 5-bromobenzotriazole and 5,6-dibromobenzotriazole are most probably differently oriented in the ATP binding site, as qualitatively confirmed by tyrosine quenching (Winiewska *et al.*, 2015a).

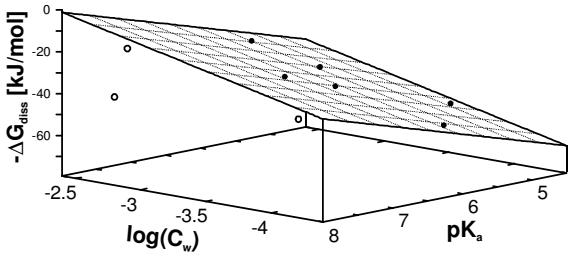

Figure 5. Correlation between the aqueous solubility (Cw) and pK_a for dissociation with binding affinity to protein kinase CK2α for a series of nine benzotriazoles halogenated on the benzene ring. Data for three ligands (open circles), pK_a for which is close to the physiological pH, disagree with the general trend.

CONCLUSIONS

The foregoing analysis clearly shows that in the tightly packed ATP binding pocket of a protein kinase, due to observed significant differences in geometrical preferences, a pattern of H-bonds cannot *a priori* be replaced by X-bonds. However, the ATP-like H-bonding pattern to the hinge region may be replaced by two parallel X-bonds formed between backbone carbonyl groups and two halogen atoms attached to vicinal carbons of the benzene ring. This interaction with the hinge region (either *via* halogen or hydrogen bonds), when accompanied by an X-bond formed with the aromatic residue located upstream of the hinge region, may possibly be used to strengthen ligand binding, or to enhance ligand selectivity.

Apart from direct effects of halogenation: increased ligand hydrophobicity and possible X-bonding, there are additional effects. These include modulation of the electron density, pK_a changes of a dissociable group, or strengthening of H-bonds formed between a halogenated ligand and a protein. All these factors affect the binding mode, so that closely related ligands may bind in different orientations, as a result of a subtle balance of electrostatic, hydrogen-bonding and halogen-bonding interactions, with the hydrophobic and electrostatic components predominating. This makes computer-aided drug design for protein kinases extremely challenging.

ACKNOWLEDGEMENTS

This work was supported by the Polish National Science Centre grant 2012/07/B/ST4/01334.

Table 1. Short intermolecular contacts between the halogen atom of a ligand and various types of potential X-bond acceptors identified in 320 PDB structures of protein kinases with halogenated ligands. The second numbers reported in each cell represent values determined for X··Acc interactions with C-X··Acc angle > 140º.

X-bond acceptor	X-bond donor			Total	Median for X···Acc distance [Å]			Median for C-X···Acc angle [°]		
	Cl	Br	I		Cl	Br	I	Cl	Br	I
O (backbone)	88; 64	64; 52	32; 30	184; 146	3.15; 3.12	3.17; 3.12	3.30; 3.29	156; 159	158; 162	173; 173
O (side-chain)	52; 16	10; 3	6; 2	68; 21	3.05; 3.10	3.18; 3.22	3.25; 3.04	105; 158	128; 146	120; 158
O (water)*	39; 13	44; 15	7; 6	90; 34	3.13; 3.09	3.19; 3.04	3.19; 3.25	129; 164	130; 167	145; 159
N (backbone)	19; 2	6; 0	0; 0	25; 2	3.15; 3.03	3.39; -	-	127; 144	110; -	-
N (side-chain)	12; 3	1; 1	0; 0	13; 3	3.25; 3.11	3.00; 3.00	-	127; 146	165; 165	-
Aromatic side-chain	8; 3	18; 17	4; 4	30; 24	3.39; 3.30	3.89; 3.91	4.09; 4.09	133; 168	159; 160	151; 151
S (side-chain)	5; 1	5; 0	4; 4	14; 5	3.10; 3.37	3.49; -	3.65; 3.65	128; 160	84; -	154; 154
Total	223; 102	148; 88	53; 46	424; 236						

* The identity of the solvent molecule cannot be deduced with 100% certainty from X-ray crystallographic data

Table 2. Short contacts between a halogen atom and aromatic ring identified in complexes of protein kinases with halogenated ligands. All contacts marked in bold fulfill the formal definition of an X···π halogen bond.

PDB	Res [Å]	Mol	Res	Motif	Ligand	Type	proximal solvent		Aromatic residue					
							Dist [Å]	Angle	Dist [Å]			Angle		
							X··O	CX··O	X··C	X··rim	X··q	CX··q	CX··π	π··π
3nux	2.70	A	F98	< hinge	3NV	rim	3.61	96	3.30	3.44	**3.91**	**156**	77	77
3owk	1.80	A	F113	< hinge	18E	rim	3.01	127	3.27	3.24	3.64	132	35	35
4a06	2.00	A	F157	< hinge	A06	rim			3.02	3.04	3.19	130	37	85
4a07	1.85	A	F157	< hinge	AZ7	rim			2.98	2.98	3.17	134	46	83
4fv6	2.50	A	Y34	Gly-loop	E57	cen	3.87	80	3.42	3.37	**3.27**	**168**	81	81
4knb	2.40	C	Y1230	cat loop	1RU	π-π			3.37	3.36	3.47	84	10	25
4med	2.80	A	F49	Gly-loop	RTX	rim			3.16	3.25	3.64	111	40	46
4qte	1.50	A	Y36	Gly-loop	390	cen			3.44	3.37	**3.30**	**168**	74	75
1h08	1.80	A	F80	< hinge	BWP	rim	3.11	116	3.45	3.43	**4.00**	**163**	37	49
1p5e	2.22	A	F80	< hinge	TBS	rim	2.91	122	3.26	3.23	**3.49**	**154**	44	45
1p5e	2.22	C	F80	< hinge	TBS	rim	3.03	112	3.24	3.26	**3.68**	**175**	55	58
1zoe	1.77	A	F113	< hinge	K25	rim	2.87	126	3.49	3.55	**3.93**	**163**	44	47
1zog	2.30	A	F113	< hinge	K37	rim	3.14	106	3.23	3.19	**3.53**	**154**		
1zog	2.30	A	F113	< hinge	K37	rim	3.20	115	3.47	3.49	**3.87**	**159**	42	43
1zoh	1.81	A	F113	< hinge	K44	rim			3.51	3.50	**3.92**	**159**	41	42
2oxy	1.81	A	F113	< hinge	K17	rim	2.90	126	3.66	3.59	**3.91**	**154**		
2oxy	1.81	B	F113	< hinge	K17	rim	3.06	118	3.53	3.51	**3.81**	**156**	44	45
2r3j	1.65	A	F80	< hinge	SCJ	rim			3.41	3.41	**3.95**	**163**	39	60
2r3k	1.70	A	F80	< hinge	SCQ	rim			3.37	3.31	**3.91**	**163**	40	59
2r3l	1.65	A	F80	< hinge	SCW	rim			3.51	3.49	**4.05**	**160**	36	57
2r3q	1.35	A	F80	< hinge	5SC	rim	3.01	154	3.52	3.55	**3.96**	**155**	35	51
3kxh	1.70	A	F113	< hinge	K66	rim			3.35	3.38	**3.53**	**165**	57	59
3kxm	1.75	A	F113	< hinge	K74	rim	3.02	117	3.49	3.50	**3.81**	**155**	42	42
3vqh	1.95	A	F54	Gly-loop	IQB	rim			3.26	3.24	**3.70**	**162**	65	65
4bxa	1.75	A	F113	< hinge	JRJ	rim			3.47	3.47	**3.97**	**163**	42	44
4c37	1.70	A	Y54	Gly-loop	Z21	rim	3.19	117	3.50	3.54	3.75	116	30	41
2vuw	1.80	A	F605	< hinge	5ID	rim	3.71	137	3.52	3.60	**4.14**	**153**	43	47
3iq7	2.00	A	F605	< hinge	5ID	rim	3.78	134	3.53	3.62	**4.12**	**151**	46	52
4mne	2.85	H	H87	cat loop	573	rim			3.53	3.53	**3.82**	**141**	52	61
4ouc	1.90	A	F605	< hinge	5ID	rim	3.67	139	3.59	3.63	**4.06**	**151**	43	50

REFERENCES

Aakeroey CB, Panikkattu S, Chopade PD, Desper J (2013) Competing hydrogen-bond and halogen-bond donors in crystal engineering. *CrystEngComm* **15**: 3125-3136

Anderson TW, Darling DA (1952) Asymptotic theory of certain goodness of fit criteria based on stochastic processes. *Ann. Math. Stat.* **23**: 193-212

Auffinger P, Hays FA, Westhof E, Ho PS (2004) Halogen bonds in biological molecules. *Proc. Natl. Acad. Sci. U. S. A.* **101**: 16789-16794

Barratt E, Bingham RJ, Warner DJ, Laughton CA, Phillips SEV, Homans SW (2005) Van der waals interactions dominate ligand-protein association in a protein binding site occluded from solvent water. *J. Am. Chem. Soc.* **127**: 11827-11834

Battistutta R, De Moliner E, Sarno S, Zanotti G, Pinna LA (2001) Structural features underlying selective inhibition of protein kinase CK2 by ATP site-directed tetrabromo-2-benzotriazole. *Protein Sci.* **10**: 2200-2206

Battistutta R, Mazzorana M, Sarno S, Kazimierczuk Z, Zanotti G, Pinna LA (2005) Inspecting the structure-activity relationship of protein kinase CK2 inhibitors derived from tetrabromo-benzimidazole. *Chem. Biol.* **12**: 1211-1219

Battistutta R, Mazzorana M, Cendron L, Bortolato A, Sarno S, Kazimierczuk Z, Zanotti G, Moro S, Pinna LA (2007) The ATP-binding site of protein kinase CK2 holds a positive electrostatic area and conserved water molecules. *ChemBioChem* **8**: 1804-1809

Battistutta R (2009) Structural bases of protein kinase CK2 inhibition. *Cell. Mol. Life Sci.* **66**: 1868-1889

Beale TM, Chudzinski MG, Sarwar MG, Taylor MS (2013) Halogen bonding in solution: thermodynamics and applications. *Chem. Soc. Rev.* **42**: 1667-1680

Besant PG, Tan E, Attwood PV (2003) Mammalian protein histidine kinases. *Int. J. Biochem. Cell Biol.* **35**: 297-309

Besant PG, Attwood PV (2005) Mammalian histidine kinases. *BBA-Proteins and Proteomics* **1754**: 281-290

Besant PG, Attwood PV, Piggott MJ (2009) Focus on Phosphoarginine and Phospholysine. *Curr. Protein Peptide Sci.* **10**: 536-550

Bogoyevitch MA, Fairlie DP (2007) A new paradigm for protein kinase inhibition: blocking phosphorylation without directly targeting ATP binding. *Drug Discov. Today* **12**: 622-633

Bondi A (1964) van der Waals volumes and radii. *J. Phys. Chem.* **68**: 441-451

Cabrita MT, Vale C, Rauter AP (2010) Halogenated Compounds from Marine Algae. *Mar. Drugs* **8**: 2301-2317

Carlsson AC, Veiga AX, Erdélyi M (2015) Halogen Bonding in Solution. *Top. Curr. Chem.*

Carter M, Ho PS (2011) Assaying the Energies of Biological Halogen Bonds. *Cryst. Growth Des.* **11**: 5087-5095

Chaikuad A, Tacconi EM, Zimmer J, Liang Y, Gray NS, Tarsounas M, Knapp S (2014) A unique inhibitor binding site in ERK1/2 is associated with slow binding kinetics. *Nat. Chem. Biol.* **10**: 853-860

Ciesla J, Fraczyk T, Rode W (2011) Phosphorylation of basic amino acid residues in proteins: important but easily missed. *Acta Biochim. Pol.* **58**: 137-147

Clark T, Hennemann M, Murray JS, Politzer P (2007) Halogen bonding: the sigma-hole. *J. Mol. Model.* **13**: 291-296

Cohen P (2002) Protein kinases - the major drug targets of the twenty-first century? *Nat. Rev. Drug Discov.* **1**: 309-315

Couty S, Westwood IM, Kalusa A, Cano C, Travers J, Boxall K, Chow CL, Burns S, Schmitt J, Pickard L, Barillari C, McAndrew PC, Clarke PA, Linardopoulos S, Griffin RJ, Aherne GW, Raynaud FI, Workman P, Jones K, van Montfort RL (2013) The discovery of potent ribosomal S6 kinase inhibitors by high-throughput screening and structure-guided drug design. *Oncotarget* **4**: 1647-1661

Cowan-Jacob SW, Jahnke W, Knapp S (2014) Novel approaches for targeting kinases: allosteric inhibition, allosteric activation and pseudokinases. *Future Med. Chem.* **6**: 541-561

Cozza G, Girardi C, Ranchio A, Lolli G, Sarno S, Orzeszko A, Kazimierczuk Z, Battistutta R, Ruzzene M, Pinna LA (2014) Cell-permeable dual inhibitors of protein kinases CK2 and PIM-1: structural features and pharmacological potential. *Cell. Mol. Life Sci.* **71**: 3173-3185

Das K, Clark AD, Lewi PJ, Heeres J, de Jonge MR, Koymans LMH, Vinkers HM, Daeyaert F, Ludovici DW, Kukla MJ, De Corte B, Kavash RW, Ho CY, Ye H, Lichtenstein MA, Andries K, Pauwels R, de Bethune MP,

Boyer PL, Clark P, Hughes SH, Janssen PAJ, Arnold E (2004) Roles of conformational and positional adaptability in structure-based design of TMC125-R165335 (etravirine) and related non-nucleoside reverse transcriptase inhibitors that are highly potent and effective against wild-type and drug-resistant HIV-1 variants. *J. Med. Chem.* **47**: 2550-2560

De Moliner E, Brown NR, Johnson LN (2003) Alternative binding modes of an inhibitor to two different kinases. *Eur. J. Biochem.* **270**: 3174-3181

DeLano WL, Lam JW (2005) PyMOL: A communications tool for computational models. *Abstr. Pap. Am. Chem. Soc.* **230**: U1371-U1372

Desiraju GR, Ho PS, Kloo L, Legon AC, Marquardt R, Metrangolo P, Politzer P, Resnati G, Rissanen K (2013) Definition of the halogen bond (IUPAC Recommendations 2013). *Pure Appl. Chem.* **85**: 1711-1713

Dietrich J, Hulme C, Hurley LH (2010) The design, synthesis, and evaluation of 8 hybrid DFG-out allosteric kinase inhibitors: A structural analysis of the binding interactions of Gleevec (R), Nexavar (R), and BIRB-796. *Biorg. Med. Chem.* **18**: 5738-5748

Dunitz JD (2004) Organic fluorine: Odd man out. ChemBioChem **5:** 614-621

Eckenhoff RG, Johansson JS (1997) Molecular interactions between inhaled anesthetics and proteins. *Pharmacol. Rev.* **49**: 343-367

Elsholz AKW, Turgay K, Michalik S, Hessling B, Gronau K, Oertel D, Maeder U, Bernhardt J, Becher D, Hecker M, Gerth U (2012) Global impact of protein arginine phosphorylation on the physiology of Bacillus subtilis. *Proc. Natl. Acad. Sci. U. S. A.* **109**: 7451-7456

Emsley P, Cowtan K (2004) Coot: model-building tools for molecular graphics. *Acta Crystallogr. Sect. D. Biol. Crystallogr.* **60**: 2126-2132

Emsley P, Lohkamp B, Scott WG, Cowtan K (2010) Features and development of Coot. *Acta Crystallogr. Sect. D. Biol. Crystallogr.* **66**: 486-501

Fabbro D (2015) 25 Years of Small Molecular Weight Kinase Inhibitors: Potentials and Limitations. *Mol. Pharmacol.* **87**: 766-775

Feng J, Zhu M, Schaub MC, Gehrig P, Roschitzki B, Lucchinetti E, Zaugg M (2008) Phosphoproteome analysis of isoflurane-protected heart mitochondria: phosphorylation of adenine nucleotide translocator-1 on Tyr(194) regulates mitochondrial function. *Cardiovasc. Res.* **80**: 20-29

Fischer PM (2004) The design of drug candidate molecules as selective inhibitors of therapeutically relevant protein kinases. *Curr. Med. Chem.* **11**: 1563-1583

Fischmann TO, Smith CK, Mayhood TW, Myers JE, Reichert P, Mannarino A, Carr D, Zhu H, Wong J, Yang RS, Le HV, Madison VS (2009) Crystal structures of MEK1 binary and ternary complexes with nucleotides and inhibitors. *Biochemistry* **48**: 2661-2674

Fuhrmann J, Schmidt A, Spiess S, Lehner A, Turgay K, Mechtler K, Charpentier E, Clausen T (2009) McsB Is a Protein Arginine Kinase That Phosphorylates and Inhibits the Heat-Shock Regulator CtsR. *Science* **324**: 1323-1327

Garuti L, Roberti M, Bottegoni G (2010) Non-ATP Competitive Protein Kinase Inhibitors. *Curr. Med. Chem.* **17**: 2804-2821

Goldstein DM, Soth M, Gabriel T, Dewdney N, Kuglstatter A, Arzeno H, Chen J, Bingenheimer W, Dalrymple SA, Dunn J, Farrell R, Frauchiger S, La Fargue J, Ghate M, Graves B, Hill RJ, Li FJ, Litman R, Loe B, McIntosh J, McWeeney D, Papp E, Park J, Reese HF, Roberts RT, Rotstein D, Pablo BS, Sarma K, Stahl M, Sung ML, Suttman RT, Sjogren EB, Tan YC, Trejo A, Welch M, Weller P, Wong BR, Zecic H (2011) Discovery of 6-(2,4-Difluorophenoxy)-2 3-hydroxy-1-(2-hydroxyethyl)propylamino -8-met hyl-8H-pyrido 2,3-d pyrimidin-7-one (Pamapimod) and 6-(2,4-Difluorophenoxy)-8-methyl-2-(tetrahydro-2H-pyran-4-ylamino) pyrido 2,3-d pyrimidin-7(8H)-one (R1487) as Orally Bioavailable and Highly Selective Inhibitors of p38 alpha Mitogen-Activated Protein Kinase. *J. Med. Chem.* **54**: 2255-2265

Gower CM, Chang MEK, Maly DJ (2014) Bivalent inhibitors of protein kinases. *Crit. Rev. Biochem. Mol. Biol.* **49**: 102-115

Hardegger LA, Kuhn B, Spinnler B, Anselm L, Ecabert R, Stihle M, Gsell B, Thoma R, Diez J, Benz J, Plancher J-M, Hartmann G, Banner DW, Haap W, Diederich F (2011) Systematic Investigation of Halogen Bonding in Protein-Ligand Interactions. *Angew. Chem. Int. Ed.* **50**: 314-318

Harrison S, Das K, Karim F, Maclean D, Mendel D (2008) Non-ATP-competitive kinase inhibitors - enhancing selectivity through new inhibition strategies. *Expert Opin. Drug Discovery* **3**: 761-774

Hauchecorne D, van der Veken BJ, Moiana A, Herrebout WA (2010) The C-Cl···N halogen bond, the weaker relative of the C···I and **C-**Br···N halogen bonds, finally characterized in solution. *Chem. Phys.* **374**: 30-36

Hendsch ZS, Tidor B (1994) Do salt bridges stabilize proteins? A continuum electrostatic analysis. *Protein Sci.* **3**: 211-226

Hernandes MZ, Cavalcanti SMT, Moreira DRM, de Azevedo WF, Jr., Lima Leite AC (2010) Halogen Atoms in the Modern Medicinal Chemistry: Hints for the Drug Design. *Curr. Drug Targets* **11**: 303-314

Howard JAK, Hoy VJ, OHagan D, Smith, GT (1996) How good is fluorine as a hydrogen bond acceptor? Tetrahedron **52:** 12613-12622

Hubig SM, Lindeman SV, Kochi JK (2000) Charge-transfer bonding in metal-arene coordination. *Coord. Chem. Rev.* **200**: 831-873

Ibrahim MAA (2011) Molecular Mechanical Study of Halogen Bonding in Drug Discovery. *J. Comput. Chem.* **32**: 2564-2574

Ibrahim MAA (2012) AMBER Empirical Potential Describes the Geometry and Energy of Noncovalent Halogen Interactions Better than Advanced Semiempirical Quantum Mechanical Method PM6-DH2X. *J. Phys. Chem. B* **116**: 3659-3669

Joosten RP, Long F, Murshudov GN, Perrakis A (2014) The PDB_REDO server for macromolecular structure model optimization. *IUCrJ* **1**: 213-220

Jorgensen WL, Schyman P (2012) Treatment of Halogen Bonding in the OPLS-AA Force Field: Application to Potent Anti-HIV Agents. *J. Chem. Theory Comput.* **8**: 3895-3901

Khorasanizadeh S (2004) The nucleosome: From genomic organization to genomic regulation. *Cell* **116**: 259-272

Kirkland LO, McInnes C (2009) Non-ATP competitive protein kinase inhibitors as anti-tumor therapeutics. *Biochem. Pharmacol.* **77**: 1561-1571

Kleywegt GJ, Harris MR, Zou JY, Taylor TC, Wahlby A, Jones TA (2004) The Uppsala Electron-Density Server. *Acta Crystallogr. Sect. D. Biol. Crystallogr.* **60**: 2240-2249

Klumpp S, Krieglstein J (2002) Phosphorylation and dephosphorylation of histidine residues in proteins. *Eur. J. Biochem.* **269**: 1067-1071

Kolar M, Hobza P (2012) On Extension of the Current Biomolecular Empirical Force Field for the Description of Halogen Bonds. *J. Chem. Theory Comput.* **8**: 1325-1333

Koshland DE (1994) The key-lock theory and the induced fit theory. *Angew. Chem. Int. Ed.* **33**: 2375-2378

Kraut DA, Churchill MJ, Dawson PE, Herschlag D (2009) Evaluating the Potential for Halogen Bonding in the Oxyanion Hole of Ketosteroid Isomerase Using Unnatural Amino Acid Mutagenesis. *ACS Chem. Biol.* **4**: 269-273

Krieger E, Joo K, Lee J, Lee J, Raman S, Thompson J, Tyka M, Baker D, Karplus K (2009) Improving physical realism, stereochemistry, and side-chain accuracy in homology modeling: Four approaches that performed well in CASP8. *Proteins: Struct. Funct. Bioinform.* **77**: 114-122

Kruskal WH, Wallis WA (1952) Use of ranks in one-criterion variance analysis. *J. Amer. Statist. Assoc.* **47**: 583-621

Kuglstatter A, Wong A, Tsing S, Lee SW, Lou Y, Villaseñor AG, Bradshaw JM, Shaw D, Barnett JW, Browner MF (2011) Insights into the conformational flexibility of Bruton's tyrosine kinase from multiple ligand complex structures. *Protein Sci.* **20**: 428-436

Lamba V, Ghosh I (2012) New Directions in Targeting Protein Kinases: Focusing Upon True Allosteric and Bivalent Inhibitors. *Curr. Pharm. Des.* **18**: 2936-2945

Lapek JD, Jr., Tombline G, Kellersberger KA, Friedman MR, Friedman AE (2015) Evidence of histidine and aspartic acid phosphorylation in human prostate cancer cells. *Naunyn-Schmiedeberg's Arch. Pharmacol.* **388**: 161-173

Lepsik M, Rezac J, Kolar M, Pecina A, Hobza P, Fanfrlik J (2013) The Semiempirical Quantum Mechanical Scoring Function for In Silico Drug Design. *ChemPlusChem* **78**: 921-931

Li H, Lu Y, Liu Y, Zhu X, Liu H, Zhu W (2012) Interplay between halogen bonds and pi-pi stacking interactions: CSD search and theoretical study. *Phys. Chem. Chem. Phys.* **14**: 9948-9955

Liu Q, Sabnis Y, Zhao Z, Zhang T, Buhrlage SJ, Jones LH, Gray NS (2013) Developing Irreversible Inhibitors of the Protein Kinase Cysteinome. *Chem. Biol.* **20**: 146-159

Liu RY, Loll PJ, Eckenhoff RG (2005) Structural basis for high-affinity volatile anesthetic binding in a natural 4-helix bundle protein. *FASEB J.* **19**: 567-576

Lu Y-X, Zou J-W, Wang Y-H, Yu Q-S (2006) Bifurcated halogen bonds: An ab initio study of the three-center interactions. *J. Mol. Struct. Theochem* **767**: 139-142

Lu YX, Shi T, Wang Y, Yang HY, Yan XH, Luo XM, Jiang HL, Zhu WL (2009) Halogen Bonding-A Novel Interaction for Rational Drug Design? *J. Med. Chem.* **52**: 2854-2862

Mann HB, Whitney DR (1947) On a test of whether one of two random variables is stochastically larger than the other. *Ann. Math. Stat.* **18**: 50-60

Massey FJ (1951) The distribution of the maximum deviation between 2 sample cumulative step functions. *Ann. Math. Stat.* 22: 125-128

Matthews HR (1995) Protein-kinases and phosphatases that act on histidine, lysine, or arginine residues in eukaryotic proteins - a possible regulator of the mitogen-activated protein-kinase cascade. *Pharmacol. Ther.* **67**: 323-350

Memic A, Spaller MR (2008) How Do Halogen Substituents Contribute to Protein-Binding Interactions? A Thermodynamic Study of Peptide Ligands with Diverse Aryl Halides. *ChemBioChem* **9**: 2793-2795

Metrangolo P, Neukirch H, Pilati T, Resnati G (2005) Halogen bonding based recognition processes: A world parallel to hydrogen bonding. *Acc. Chem. Res.* **38**: 386-395

Metrangolo P, Meyer F, Pilati T, Resnati G, Terraneo G (2008) Halogen bonding in supramolecular chemistry. *Angew. Chem. Int. Ed.* **47**: 6114-6127

Nazare M, Will DW, Matter H, Schreuder H, Ritter K, Urmann M, Essrich M, Bauer A, Wagner M, Czech J, Lorenz M, Laux V, Wehner V (2005) Probing the subpockets of factor Xa reveals two binding modes for inhibitors based on a 2-carboxyindole scaffold: A study combining structure-activity relationship and X-ray crystallography. *J. Med. Chem.* **48**: 4511-4525

Niefind K, Raaf J, Issinger OG (2009) Protein kinase CK2: From structures to insights. *Cell. Mol. Life Sci.* **66**: 1800-1816

Novak M, Foroutan-Nejad C, Marek R (2015) Asymmetric bifurcated halogen bonds. *Phys. Chem. Chem. Phys.* **17**: 6440-6450

Pannifer ADB, Flint AJ, Tonks NK, Barford D (1998) Visualization of the cysteinyl-phosphate intermediate of a protein-tyrosine phosphatase by X-ray crystallography. *J. Biol. Chem.* **273**: 10454-10462

Parang K, Till JH, Ablooglu AJ, Kohanski RA, Hubbard SR, Cole PA (2001) Mechanism-based design of a protein kinase inhibitor. *Nat. Struct. Biol.* **8**: 37-41

Parang K, Cole PA (2002) Designing bisubstrate analog inhibitors for protein kinases. *Pharmacol. Ther.* **93**: 145-157

Parisini E, Metrangolo P, Pilati T, Resnati G, Terraneo G (2011) Halogen bonding in halocarbon-protein complexes: a structural survey. *Chem. Soc. Rev.* **40**: 2267-2278

Pauletti PM, Cintra LS, Braguine CG, da Silva Filho AA, Andrade e Silva ML, Cunha WR, Januario AH (2010) Halogenated Indole Alkaloids from Marine Invertebrates. *Mar. Drugs* **8**: 1526-1549

Persch E, Dumele O, Diederich F (2015) Molecular Recognition in Chemical and Biological Systems. *Angew. Chem. Int. Ed.* **54**: 3290-3327

Pflug A, Johnson KA, Engh RA (2012) Anomalous dispersion analysis of inhibitor flexibility: a case study of the kinase inhibitor H-89. *Acta Crystallogr. Sect. F Struct. Biol. Cryst. Commun.* **68**: 873-877

Politzer P, Murray JS, Concha MC (2007) Halogen bonding and the design of new materials: organic bromides, chlorides and perhaps even fluorides as donors. *J. Mol. Model.* **13**: 643-650

Poznanski J, Najda A, Bretner M, Shugar D (2007) Experimental (C-13 NMR) and theoretical (ab initio molecular orbital calculations) studies on the prototropic tautomerism of benzotriazole and some derivatives symmetrically substituted on the benzene ring. *J. Phys. Chem. A* **111**: 6501-6509

Poznanski J, Shugar D (2013) Halogen bonding at the ATP binding site of protein kinases: Preferred geometry and topology of ligand binding. *BBA-Proteins and Proteomics* **1834**: 1381-1386

Poznanski J, Poznanska A, Shugar D (2014) A Protein Data Bank Survey Reveals Shortening of Intermolecular Hydrogen Bonds in Ligand-Protein Complexes When a Halogenated Ligand Is an H-Bond Donor. *PLoS One* **9**: e99984

Reddy DS, Craig DC, Desiraju GR (1996) Supramolecular synthons in crystal engineering .4. Structure simplification and synthon interchangeability in some organic diamondoid solids. *J. Am. Chem. Soc.* **118**: 4090-4093

Rendine S, Pieraccini S, Forni A, Sironi M (2011) Halogen bonding in ligand-receptor systems in the framework of classical force fields. *Phys. Chem. Chem. Phys.* **13**: 19508-19516

Richardson CM, Williamson DS, Parratt MJ, Borgognoni J, Cansfield AD, Dokurno P, Francis GL, Howes R, Moore JD, Murray JB, Robertson A, Surgenor AE, Torrance CJ (2006) Triazolo[1,5-a]pyrimidines as novel CDK2 inhibitors: protein structure-guided design and SAR. *Bioorg. Med. Chem. Lett.* **16**: 1353-1357

Robarge KD, Lee W, Eigenbrot C, Ultsch M, Wiesmann C, Heald R, Price S, Hewitt J, Jackson P, Savy P, Burton B, Choo EF, Pang J, Boggs J, Yang A, Yang X, Baumgardner M (2014) Structure based design of novel 6,5 heterobicyclic mitogen-activated protein kinase kinase (MEK) inhibitors leading to the discovery of imidazo[1,5-a] pyrazine G-479. *Bioorg. Med. Chem. Lett.* **24**: 4714-4723

Rosokha SV, Kochi JK (2008) X-ray structures and electronic spectra of the pi-halogen complexes between halogen donors and acceptors with pi-receptors. *Halogen Bonding: Fundamentals and Applications* **126**: 137-160

Sarno S, Papinutto E, Franchin C, Bain J, Elliott M, Meggio F, Kazimierczuk Z, Orzeszko A, Zanotti G, Battistutta R, Pinna LA (2011) ATP Site-Directed Inhibitors of Protein Kinase CK2: An Update. *Curr. Top. Med. Chem.* **11**: 1340-1351

Sarwar MG, Dragisic B, Salsberg LJ, Gouliaras C, Taylor MS (2010) Thermodynamics of Halogen Bonding in Solution: Substituent, Structural, and Solvent Effects. *J. Am. Chem. Soc.* **132**: 1646-1653

Scholfield MR, Vander Zanden CM, Carter M, Ho PS (2013) Halogen bonding (X-bonding): A biological perspective. *Protein Sci.* **22**: 139-152

Schulze-Gahmen U, DeBondt HL, Kim SH (1996) High-resolution crystal structures of human cyclin-dependent kinase 2 with and without ATP: Bound waters and natural ligand as guides for inhibitor design. *J. Med. Chem.* **39**: 4540-4546

Smit AJ (2004) Medicinal and pharmaceutical uses of seaweed natural products: A review. *J. Appl. Phycol.* **16**: 245-262

Steeg PS, Palmieri D, Ouatas T, Salerno M (2003) Histidine kinases and histidine phosphorylated proteins in mammalian cell biology, signal transduction and cancer. *Cancer Lett.* **190**: 1-12

Steinig AG, Li AH, Wang J, Chen X, Dong H, Ferraro C, Jin M, Kadalbajoo M, Kleinberg A, Stolz KM, Tavares-Greco PA, Wang T, Albertella MR, Peng Y, Crew L, Kahler J, Kan J, Schulz R, Cooke A, Bittner M, Turton RW, Franklin M, Gokhale P, Landfair D, Mantis C, Workman J, Wild R, Pachter J, Epstein D, Mulvihill MJ (2013) Novel 6-aminofuro[3,2-c]pyridines as potent, orally efficacious inhibitors of cMET and RON kinases. *Bioorg. Med. Chem. Lett.* **23**: 4381-4387

Tong YS, Lin NH, Wang L, Hasvold L, Wang WB, Leonard N, Li TM, Li Q, Cohen J, Gu WZ, Zhang HY, Stoll V, Bauch J, Marsh K, Rosenberg SH, Sham HL (2003) Discovery of potent imidazole and cyanophenyl containing farnesyltransferase inhibitors with improved oral bioavailability. *Bioorg. Med. Chem. Lett.* **13**: 1571-1574

Ventimig.Fa, Wool IG (1974) Kinase that transfers gamma-phosphoryl group of gtp to proteins of eukaryotic 40s ribosomal-subunits. *Proc. Natl. Acad. Sci. U. S. A.* **71**: 350-354

Voth AR, Hays FA, Ho PS (2007) Directing macromolecular conformation through halogen bonds. *Proc. Natl. Acad. Sci. U. S. A.* **104**: 6188-6193

Voth AR, Ho PS (2007) The role of halogen bonding in inhibitor recognition and binding by protein kinases. *Curr. Top. Med. Chem.* **7**: 1336-1348

Voth AR, Khuu P, Oishi K, Ho PS (2009) Halogen bonds as orthogonal molecular interactions to hydrogen bonds. *Nat. Chem.* **1**: 74-79

Wagner PD, Vu ND (2000) Histidine to aspartate phosphotransferase activity of nm23 proteins: phosphorylation of aldolase C on Asp-319. *Biochem. J.* **346**: 623-630

Wang L, Gao J, Bi F, Song B, Liu C (2014) Toward the Development of the Potential with Angular Distortion for Halogen Bond: A Comparison of Potential Energy Surfaces between Halogen Bond and Hydrogen Bond. *J. Phys. Chem. A* **118**: 9140-9147

Wang W, Okada Y, Shi HB, Wang YQ, Okuyama T (2005) Structures and aldose reductase inhibitory effects of bromophenols from the red alga Symphyocladia latiuscula. *J. Nat. Prod.* **68**: 620-622

Wasik R, Lebska M, Felczak K, Poznanski J, Shugar D (2010) Relative Role of Halogen Bonds and Hydrophobic Interactions in Inhibition of Human Protein Kinase CK2 alpha by Tetrabromobenzotriazole and Some C(5)-Substituted Analogues. *J. Phys. Chem. B* **114**: 10601-10611

Wasik R, Winska P, Poznanski J, Shugar D (2012a) Synthesis and Physico-Chemical Properties in Aqueous Medium of All Possible Isomeric Bromo Analogues of Benzo-1H-Triazole, Potential Inhibitors of Protein Kinases. *J. Phys. Chem. B* **116**: 7259-7268

Wasik R, Winska P, Poznanski J, Shugar D (2012b) Isomeric Mono-, Di-, and Tri-Bromobenzo-1H-Triazoles as Inhibitors of Human Protein Kinase CK2 alpha. *PLoS One* **7**: e48898

Wenglowsky S, Ren L, Ahrendt KA, Laird ER, Aliagas I, Alicke B, Buckmelter AJ, Choo EF, Dinkel V, Feng B, Gloor SL, Gould SE, Gross S, Gunzner-Toste J, Hansen JD, Hatzivassiliou G, Liu B, Malesky K, Mathieu S, Newhouse B, Raddatz NJ, Ran Y, Rana S, Randolph N, Risom T, Rudolph J, Savage S, Selby LT, Shrag M, Song K, Sturgis HL, Voegtli WC, Wen Z, Willis BS, Woessner RD, Wu WI, Young WB, Grina J (2011) Pyrazolopyridine Inhibitors of B-Raf(V600E). Part 1: The Development of Selective, Orally Bioavailable, and Efficacious Inhibitors. *ACS Med. Chem. Lett.* **2**: 342-347

Wilcken R, Zimmermann MO, Lange A, Joerger AC, Boeckler FM (2013) Principles and Applications of Halogen Bonding in Medicinal Chemistry and Chemical Biology. *J. Med. Chem.* **56**: 1363-1388

Winiewska M, Kucińska K, Makowska M, Poznański J, Shugar D (2015a) Thermodynamics parameters for binding of halogenated benzotriazole inhibitors of human protein kinase CK2α. *Biochim. Biophys. Acta*

Winiewska M, Makowska M, Maj P, Wielechowska M, Bretner M, Poznanski J, Shugar D (2015b) Thermodynamic parameters for binding of some halogenated inhibitors of human protein kinase CK2. *Biochem. Biophys. Res. Commun.* **456**: 282-287

Yasuda H, Park E, Yun CH, Sng NJ, Lucena-Araujo AR, Yeo WL, Huberman MS, Cohen DW, Nakayama S, Ishioka K, Yamaguchi N, Hanna M, Oxnard GR, Lathan CS, Moran T, Sequist LV, Chaft JE, Riely GJ, Arcila ME, Soo RA, Meyerson M, Eck MJ, Kobayashi SS, Costa DB (2013) Structural, biochemical, and clinical characterization of epidermal growth factor receptor (EGFR) exon 20 insertion mutations in lung cancer. *Sci. Transl. Med.* **5**: 216ra177

Zhang JM, Yang PL, Gray NS (2009) Targeting cancer with small molecule kinase inhibitors. *Nat. Rev. Cancer* **9**: 28-39

Zhao Z, Wu H, Wang L, Liu Y, Knapp S, Liu QS, Gray NS (2014) Exploration of Type II Binding Mode: A Privileged Approach for Kinase Inhibitor Focused Drug Discovery? *ACS Chem. Biol.* **9**: 1230-1241

Zien P, Bretner M, Zastapilo K, Szyszka R, Shugar D (2003) Selectivity of 4,5,6,7-tetrabromobenzimidazole as an ATP-competitive potent inhibitor of protein kinase CK2 from various sources. *Biochem. Biophys. Res. Commun.* **306**: 129-133

Zou WS, Han J, Jin WJ (2009) Concentration-dependent Br···O halogen bonding between carbon tetrabromide and oxygen-containing organic solvents. *J. Phys. Chem. A* **113**: 10125-10132

FIGURE LEGENDS

Figure 1. The structural analogy between a halogen (A) and a hydrogen (B) bond.

Figure 2. Representative structures of protein kinases in complexes with halogenated ligands that display short contacts between a halogen atom and a protein: (A,B) contacts orthogonal to the peptide bond; (C,D) an unusual interaction between a halogen atom and a proximal aspartate side-chain carboxyl; (E,F) π-π interaction between aromatic rings; (G,H) parallel orientation of the C-X bond relative to the aromatic ring; (I-L) halogen bonds between the ligand and an aromatic ring; (M,N) alternative binding modes of TBBt by two closely related protein kinases, and (N-P) closely related halogenated ligands that substantially differ in their location at the ATP-binding site of protein kinase CK2α; (Q) hydrogen bonding pattern with ATP; (R-T) short contacts between a halogen atom and a solvent molecule. The original pdb codes and protein acronyms are denoted for each structure. The figure includes EDS generated 2*Fo-Fc* (grey) and *Fo-Fc* (red - negative, green - positive) electron density maps contoured at given rmsd levels (inaccessible for 1j91). The short contacts with the halogen atoms are colored grey and the hydrogen bonds in yellow. The halogen atoms are colored green. The glycine-rich loop, hinge region, catalytic loop and DFG motif are denoted in magenta, yellow, red and blue, respectively.

Figure 3. Schematic representation of perpendicular "over the center" (A), "over the rim" (B) and parallel (C) orientations of bromomethane relative to a proximal benzene aromatic ring.

Figure 4. Cumulative distributions of the parameters describing the geometry of an interaction between a halogenated ligand and a backbone carbonyl (A-C,I), side-chain oxygen (D-F) and a water molecule (G-H), determined separately for each halogen type. As a reference, the distributions for an H-bond between a non-halogenated ligand and a backbone carbonyl are presented as black lines in (B,C,I), and additionally are shown for non-halogenated (HL), fluorinated (FL) and otherwise halogenated (XL) ligands acting either as donors (J-L) or acceptors (M-O) of an H-bond. Chopped lines in (A-H) represent cumulative distributions obtained for θ^X restricted to the range of 140-180º, indicative of X-bond formation, which is denoted by vertical arrows (B,E,F).

Figure 5. Correlation between the aqueous solubility (Cw) and pK_a for dissociation with binding affinity to protein kinase CK2α for a series of nine benzotriazoles halogenated on the benzene ring. Data for three ligands (open circles), pK_a for which is close to the physiological pH, disagree with the general trend.